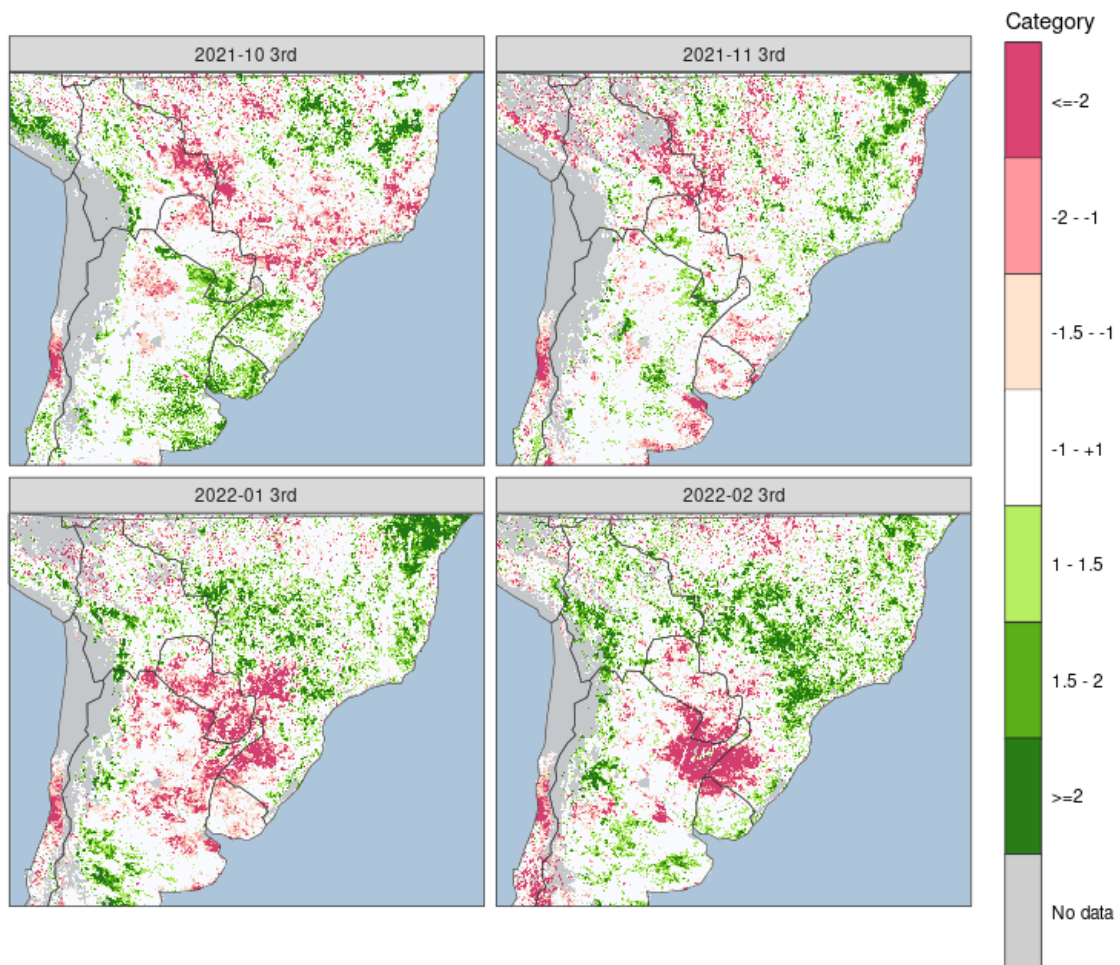


## FAPAR and FAPAR Anomaly (VIIRS)

The Copernicus Global Drought Observatory (GDO) uses the Fraction of Absorbed Photosynthetically Active Radiation (FAPAR) to detect and monitor the impacts of agricultural drought on the growth and productivity of vegetation. This Factsheet provides an overview of the VIIRS (Visible Infrared Imaging Radiometer Suite) FAPAR and FAPAR Anomaly products.

Variable	Temporal scale	Spatial scale	Coverage
Fraction of Absorbed Photosynthetically Active Radiation (FAPAR)	10 days	1/12 degree	Global



**Figure 1:** FAPAR Anomaly maps over central South America during the warm season 2021-2022 (October, November, January and February).

## 1. Brief overview of the indicator

The incoming solar radiation in the spectral range from 400 to 700 nanometers is known as Photosynthetically Active Radiation (PAR; Mottus et al., 2012). PAR provides the energy required by the terrestrial vegetation to produce organic material from mineral components (photosynthesis). The fraction of PAR that is actually absorbed by vegetation is known as the **Fraction of Absorbed Photosynthetically Active Radiation (FAPAR; Gobron and Verstraete, 2009)**.

FAPAR is a biophysical dimensionless quantity (its values range from 0/no absorption to 1/total absorption) used to assess the greenness and health of vegetation. Because of its critical role in tracing mass and energy exchanges (Chen et al., 2020), FAPAR is an input in many hydrological, climatological, agricultural and ecological models (Bayat et al., 2021) and it is recognized by the Global Climate Observing System (GCOS) as one of the Essential Climate Variables (ECV) that critically contribute to the characterization of Earth's climate (GCOS, 2016; Pettorelli et al., 2016).

During the recent decades, an increasing number of Earth observation satellites has made the release of different remote sensed FAPAR products possible. These include the MODerate resolution Imaging Spectroradiometer (MODIS), the Visible Infrared Imaging Radiometer Suite (VIIRS), the Multiangle Imaging SpectroRadiometer (MISR) and the Sentinel-3 Ocean and Land Colour Instrument (OLCI) products. Due to different FAPAR definitions, assumptions, retrieval algorithms and satellite sensors, these FAPAR products can vary substantially from each other, requiring significant data consolidation efforts to establish a continuous time series of consistent FAPAR observations and caution in determining reference values. For more details, please see among others, Chen et al. (2020) and Zhang et al. (2020).

For the assessment of agricultural drought, the Global Drought Observatory provides two different FAPAR datasets, one based on MODIS and the other on VIIRS. Both of them provide spatial and temporal time series of FAPAR that can be used to monitor the Earth's vegetation status and infer the impacts of agricultural drought on it. The MODIS dataset covers the period from January 2001 to September 2022 and is not updated any longer. The VIIRS dataset extends from January 2012 onward and is the focus of this technical document.

## 2. What the indicator shows

FAPAR anomalies can be used as an indicator to detect and monitor the impacts of agricultural drought on the growth and productivity of vegetation. The rationale behind the use of FAPAR anomalies is that rainfall deficit can result in changes in absorbed photosynthetic radiation by plants (Peng et al., 2019). Gobron et al. (2005) used multi-annual time series of FAPAR anomalies to assess the dramatic impact of the 2003 drought on plant productivity in Europe and document the recovery of the vegetation in 2004. Peng et al. (2019) used FAPAR anomalies to monitor the spatial and temporal variation of the 2005 drought in Australia. The European Drought Observatory integrates FAPAR, precipitation and soil moisture anomalies within the Combined Drought Indicator for providing an early warning system and monitoring droughts (Cammalleri et al., 2021).

FAPAR and FAPAR anomalies datasets come as raster files for every 10-day interval. The deviation of the FAPAR values from the long-term mean (anomaly) are calculated at each spatial location (grid-cell), with a reference baseline that ranges from the year 2012 to the last available full year (see Section 3). Negative FAPAR anomalies suggest conditions of relative vegetation stress, especially plant water stress due to drought, during that 10-day interval. In contrast, positive FAPAR anomalies indicate relatively favorable vegetation growth conditions during that 10-day interval.

### 3. How the indicator is calculated

The FAPAR Anomaly indicator implemented in GDO is computed using the global FAPAR products from VIIRS. These datasets are freely available through the Land Processes Distributed Active Archive Center (LP DAAC; product code VNP15A2H) and are widely used by the scientific community (Xu et al., 2018).

VIIRS is an instrument aboard the NASA/NOAA Suomi NPP (National Polar-orbiting Partnership) and NOAA-20 satellites. With the purpose of providing continuity with the MODIS mission, VIIRS global observation products are generated using modified MODIS algorithms.

In order to obtain the 10-day composite FAPAR maps, first low-quality data are masked with the use of quality flags in the VIIRS product. Secondly, the 8-day composites of the VIIRS FAPAR products are interpolated to 10-day time-steps using a weighted average (inverse distance in time) of the two closest images, and a temporal smoothing is performed by means of an exponential filter ( $\alpha = 0.5$ ) of the 10-day data (Brown and Meyer, 1961). Finally, data are spatially resampled to 1/12 decimal degree starting from the original 500 m resolution.

FAPAR anomalies are calculated by comparing the 10-day composite FAPAR maps with a VIIRS-consistent baseline of FAPAR statistics (mean and standard deviation), covering the period from 2012 up to the last available full year (for example, the 2023 FAPAR anomalies must be referred to the 2012-2022 baseline). More specifically, for every 10-day period, the FAPAR anomalies are computed as follows:

$$fAPAR\ anomaly_t = \frac{X_t - \overline{X}_t}{\sigma_t}$$

where  $X_t$  is the FAPAR value for the 10-day period  $t$ ,  $\overline{X}_t$  is the corresponding long-term average and  $\sigma_t$  is the long-term standard deviation.

## 4. How to use the indicator

Figure 2 shows the GDO MapViewer with an example of FAPAR and FAPAR Anomaly maps. In GDO, the FAPAR values and their anomalies can be represented as maps or time series plots. The first ones provide information on the spatial distribution of vegetation photosynthetic activity; the second ones, its temporal evolution over long periods. While FAPAR values are dimensionless, ranging from 0 (yellow in the color bar) to 1 (green, corresponding to maximum vegetation photosynthetic activity), FAPAR anomalies are given in classes corresponding to standard deviation units, ranging from  $\leq -2$  (red in the color bar, negative anomalies) to  $\geq +2$  (green, positive anomalies).

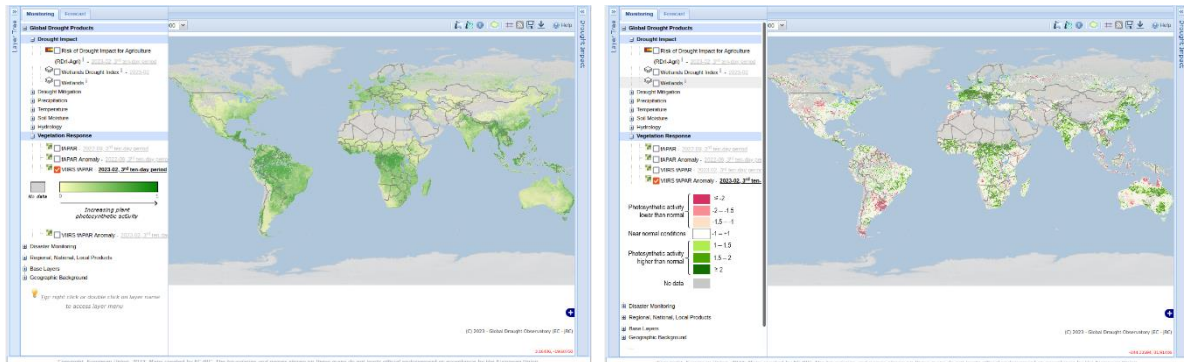


Figure 2. Maps of FAPAR values (left) and FAPAR anomalies (right) for third 10-day interval of February 2023.

## 5. Strengths and weaknesses of the indicator

### Strengths:

- FAPAR and FAPAR anomaly provide timely warnings of onset and evolution of large-scale impacts of droughts on agriculture and ecosystems.
- Every ten days, the FAPAR maps and FAPAR Anomaly maps in GDO give a spatially continuous, up-to-date picture of the vegetation productivity and/or health status, for the entire globe.
- Within GDO, gridded data are easily aggregated over administrative or natural entities such as hydrological watersheds, allowing both qualitative and quantitative comparison of the intensity and duration of FAPAR anomalies with recorded impacts such as yield reductions, low flows, reduced groundwater levels.

### Weaknesses:

- Variations in the vegetation health and/or cover could be related to stress factors not related to droughts (e.g., plant diseases, pests, hail, flooding). To determine if changes in FAPAR are linked with a drought event or not, FAPAR data should be interpreted jointly with other indicators (as in the EDO Combined Drought Indicator).
- FAPAR anomalies depend on the availability of historical time-series for the calculation of the reference mean and standard deviation. For the FAPAR Anomaly maps in GDO, it is assumed that the baseline time-series (starting in 2012) is sufficiently long to compute the long-term reference conditions. Changes in base line and base line selection criteria could affect significantly the anomaly values.

## References

- Bayat, B. and Camacho, F. and Nickeson, J. and Cosh, M. and Bolten, J. and Vereecken, H. and Montzka, C., 2021. Toward operational validation systems for global satellite-based terrestrial essential climate variables, *International Journal of Applied Earth Observation and Geoinformation*, Volume 95, <https://doi.org/10.1016/j.jag.2020.102240>.
- Brown, R.G. and R.F. Meyer., 1961. The fundamental theorem of exponential smoothing. *Operations Research*, 9 (5): 673-685. <https://www.jstor.org/stable/166814>
- Cammalleri, C. and Arias-Muñoz, C. and Barbosa, P. and de Jager, A. and Magni, D. and Masante, D. and Mazzeschi, M. and McCormick, N. and Naumann, G. and Spinoni, J. and and Vogt, J. 2021. A revision of the Combined Drought Indicator (CDI) used in the European Drought Observatory (EDO), *Nat. Hazards Earth Syst. Sci.*, 21, 481–495. <https://doi.org/10.5194/nhess-21-481-2021>
- Chen, S. and Liu, L. and He, X. and Liu, Z. and Peng, D. Upscaling from Instantaneous to Daily Fraction of Absorbed Photosynthetically Active Radiation (FAPAR) for Satellite Products. *Remote Sens.* 2020, 12, 2083. <https://doi.org/10.3390/rs12132083>
- GCOS, 2016. The Global Observing System for Climate: Implementation Needs. Technical Report GCOS-200: World Meteorological Organization. [https://unfccc.int/sites/default/files/gcos\\_ip\\_10oct2016.pdf](https://unfccc.int/sites/default/files/gcos_ip_10oct2016.pdf)
- Gobron, N. and Verstraete, M. M., 2009. Assessment of the status of the development of the standards for the Terrestrial Essential Climate Variables. FAPAR. <https://lpvs.gsfc.nasa.gov/PDF/TerrestrialECV/T10.pdf>
- Gobron, N. and Pinty, B. and Mélin, F. and Taberner, M. and Verstraete, M. M. and Belward, A. and Lavergne, T. and Widlowski, J.-L., 2005. The state of vegetation in Europe following the 2003 drought. *International Journal of Remote Sensing*, 26 (9): 2013-2020. <https://doi.org/10.1080/01431160412331330293>
- Mottus, M. and Sulev, M. and Baret, F. and Lopez-Lozano, R. and Reinart, A., 2012. Photosynthetically Active Radiation: Measurement and Modeling . In: Meyers, R.A. (eds) *Encyclopedia of Sustainability Science and Technology*. Springer, New York, NY. [https://doi.org/10.1007/978-1-4419-0851-3\\_451](https://doi.org/10.1007/978-1-4419-0851-3_451)
- Peng, J. and Muller, J.P. and Blessing, S. and Giering, R. and Danne, O. and Gobron, N. and Kharbouche, S. and Ludwig, R. and Müller, B. and Leng, G. and You, Q. and Duan, Z. and Dadson, S., 2019. Can We Use Satellite-Based FAPAR to Detect Drought? *Sensors (Basel)*. Aug 23; 19 (17):3662. doi: [10.3390/s19173662](https://doi.org/10.3390/s19173662)
- Pettorelli, N. and Wegmann, M. and Skidmore, A. and Múcher, S. and Dawson, T.P. and Fernandez, M. and Lucas, R. and Schaepman, M.E. and Wang, T. and O'Connor, B. and Jongman, R.H.G. and Kempeneers, P. and Sonnenschein, R. and Leidner, A.K. and Böhm, M. and He, K.S. and Nagendra, H. and Dubois, G. and Fatoyinbo, T. and Hansen, M.C. and Paganini, M. and de Klerk, H.M. and Asner, G.P. and Kerr, J.T. and Estes, A.B. and Schmeller, D.S. and Heiden, U. and Rocchini, D. and Pereira, H.M. and Turak, E. and Fernandez, N. and Lausch, A. and Cho, M.A. and Alcaraz-Segura, D. and McGeoch, M.A. and Turner, W. and Mueller, A. and St-Louis, V. and Penner, J. and Vihervaara, P. and Belward, A. and Reyers, B. and Geller, G.N., 2016. Framing the concept of satellite remote sensing essential biodiversity variables: challenges and future

directions. *Remote Sens Ecol Conserv*, 2: 122-131. <https://doi.org/10.1002/rse2.15>

- Zhang, Z. and Zhang, Y. and Zhang, Y. and Gobron, N. and Frankenberg, C. and Wang, S. and Li, Z., 2020. The potential of satellite FPAR product for GPP estimation: An indirect evaluation using solar-induced chlorophyll fluorescence, *Remote Sensing of Environment*, Volume 240, <https://doi.org/10.1016/j.rse.2020.111686>
- Zheng, Y. and Xiao, Z. and Li, J. and Yang, H. and Song, J., 2022. Evaluation of Global Fraction of Absorbed Photosynthetically Active Radiation (FAPAR) Products at 500 m Spatial Resolution. *Remote Sens.*, 14, 3304. <https://doi.org/10.3390/rs14143304>
- Xu, B. and Park, T. and Yan, K. and Chen, C. and Zeng, Y. and Song, W. and Yin, G. and Li, J. and Liu, Q. and Knyazikhin, Y. and Myneni, R.B., 2018. Analysis of Global LAI/FPAR Products from VIIRS and MODIS Sensors for Spatio-Temporal Consistency and Uncertainty from 2012–2016. *Forests*, 9, 73, <https://doi.org/10.3390/f9020073>

Last document update: 2023/03/29